Acta Oceanol. Sin., 2021, Vol. 40, No. 3, P. 84–93
https://doi.org/10.1007/s13131-021-1700-y
http://www.hyxb.org.cn
E-mail: hyxbe@263.net

A buried submarine canyon in the northwest South China Sea: architecture, development processes and implications for hydrocarbon exploration

Bin Wang[1], Fuliang Lyu[1], Shuang Li[2, 3, 4*], Jian Li[2, 3, 4], Zhili Yang[1], Li Li[1], Xuefeng Wang[1], Yintao Lu[1], Taotao Yang[1], Jingwu Wu[1], Guozhong Sun[1], Hongxia Ma[1], Xiaoyong Xu[1]

[1] Petrochina Hangzhou Research Institute of Geology, Hangzhou 310023, China

[2] University of Chinese Academy of Sciences, Beijing 100049, China

[3] Key Laboratory of Marginal Sea Geology, South China Sea Institute of Oceanology, Chinese Academy of Sciences, Guangzhou 510301, China

[4] Innovation Academy of South China Sea Ecology and Environmental Engineering, Chinese Academy of Sciences, Guangzhou 510301, China

Received 19 November 2019; accepted 19 March 2020

Abstract

High-resolution multichannel seismic data enables the discovery of a previous, undocumented submarine canyon (Huaguang Canyon) in the Qiongdongnan Basin, northwest South China Sea. The Huaguang Canyon with a NW orientation is 140 km in length, and 2.5 km to 5 km in width in its upper reach and 4.6 km to 9.5 km in width in its lower reach. The head of the Huaguang Canyon is close to the Xisha carbonate platform and its tail is adjacent to the central canyon. This buried submarine canyon is formed by gravity flows from the Xisha carbonate platform when the sea level dropped in the early stage of the late Miocene (~10.5 Ma). The internal architecture of the Huaguang Canyon is mainly characterized by high amplitude reflections, indicating that this ancient submarine canyon was filled with coarse-grained sediments. The sediment was principally scourced from the Xisha carbonate platform. In contrast to other buried large-scale submarine canyons (central canyon and Zhongjian Canyon) in the Qiongdongnan Basin, the Huaguang Canyon displays later formation time, smaller width and length, and single sediment supply. The coarse-grained deposits within Huaguang Canyon provide a good environment for reserving oil and gas, and the muddy fillings in Huaguang Canyon have been identified as regional caps. Therefore, Huaguang Canyon is potential area for future hydrocarbon exploration in the northwest South China Sea. Our results may contribute to a better understanding of the evolution of submarine canyons formed in carbonate environment.

Key words: South China Sea, Qiongdongnan Basin, submarine canyon, evolution

Citation: Wang Bin, Lyu Fuliang, Li Shuang, Li Jian, Yang Zhili, Li Li, Wang Xuefeng, Lu Yintao, Yang Taotao, Wu Jingwu, Sun Guozhong, Ma Hongxia, Xu Xiaoyong. 2021. A buried submarine canyon in the northwest South China Sea: architecture, development processes and implications for hydrocarbon exploration. Acta Oceanologica Sinica, 40(3): 84–93, doi: 10.1007/s13131-021-1700-y

1 Introduction

Submarine canyons are prominent topographic features on both passive and active continental margins, which can extend for thousands of kilometres across the seafloor (Harris and Whiteway, 2011). They are more common in distal slope regions and play an essential role in determining the sediment dispersal pattern and the growth of the whole fan and they are with great research value and meaning in the hydrocarbon industry (Piper and Normark, 1983; Mayall et al., 2006; McHargue et al., 2011; Ortiz-Karpf et al., 2015). Submarine canyons are very important as they could transport large volumes of sediment from the continental shelf into deep-water and form the largest sedimentary deposits on earth (Wynn et al., 2007). These deposits are significant hosts for gas and oil reserves and hold key information on past climate change and mountain building episodes. The initiation and evolution of submarine canyons result from a combination of factors, including basin tectonics, climate, sea-level changes, and Coriolis force (deviate to right in the northern hemisphere) that control the type, supply and deposition of sediment (Bouma, 2004; Kolla, 2007; Richards et al., 1998; Peakall et al., 2012; Cossu and Wells, 2013; de Leeuw et al., 2016). The research on submarine canyons is of great importance for characterizing ancient and buried turbidite units that may contain hydrocarbons (Li et al., 2013; Su et al., 2014).

Submarine canyons have been widely documented in the South China Sea where now is a promising area for hydrocarbon exploration. The cental canyon in Qiongdongnan Basin has been identified as a main hydrocarbon reservoir, which is composed of

Foundation item: The National Natural Scientific Foundation of China under contract No. 41876054; the National Science and Technology Major Project "The evaluations of deepwater oil and gas geological conditions and targets in Zhongjian area of the South China Sea" under contract No. 2017ZX05026006; the China National Petroleum Corporation (CNPC) Science and Technology Major Projects under contract Nos 2019A-1009 and 2019D-4309.
*Corresponding author, E-mail: lishuang@scsio.ac.cn

the Upper Miocene Huangliu formation (Upper Miocene) and the Pliocene Yinggehai formation (the Pliocene) (Wang, 2012; Wang et al., 2016). Moreover, large amount of gas hydrate has been found in the Zhujiang (Pearl) River Canyon system and Penghu Canyon system (Feng et al., 2015; Wang et al., 2016; Zhang et al., 2015). Studies on submarine canyons in this area, especially on the northwest South China Sea margin, has made some great progress in recent years due to the availability of high-resolution seafloor images and seismic datasets (e.g., Gong et al., 2011; Ding et al., 2013; Su et al., 2014). The most studied submarine canyon on the northwest South China margin is the central canyon, which is paralleled to the shelf break with an S-shaped geometry (Gong et al., 2011; Li et al., 2013; Su et al., 2014). Gong et al. (2011) have investigated the architecture, sequence stratigraphy and depositional processes of the central canyon. The whole canyon can be divided into three segments (the head area, the western segment and the eastern segment) based on its distinct morphological and depositional architecture characteristics (Su et al., 2014). Zhang et al. (2013) found that palaeobios buried in the central canyon are belonging to the Huangliu formation by analysing the characteristics of sedimentary microfacies, so the formation time of the central canyon is earlier than 5.5 Ma. Yuan et al. (2009) have identified a series of buried submarine canyons on the slope of Qiongdongnan Basin. These buried canyons probably developed in the late Quaternary period when a relative sea level drop occurred (Yuan et al., 2009). Turbidity currents originated from the mountain river of mid-Vietnam are proposed to contribute to the formation of these canyons (Yuan et al., 2009). Li et al. (2015) have revealed the morphology and internal architecture of numerous submarine canyons on the continental slope of Qiongdongnan Basin and they proposed that the recurrent mass-transport deposits derived from these submarine canyons could have improved the reservoir potential within the central canyon. Recently, Lu et al. (2018) reported the presence of Zhongjian Canyon between two carbonate platforms (Xisha and Guangle carbonate platforms) on the northwest South China Sea margin. They investigated the internal architecture and evolutionary processes of the Zhongjian Canyon and proposed that its formation was related to the occurrence of submarine landslides. However, few studies have investigated the submarine canyons around the Xisha carbonate platform, and their implications for hydrocarbon explorations in the northwest South China Sea.

In this paper, we identify and describe a previously, undocumented submarine canyon on the northwest South China Sea margin by utilizing high-resolution two- and three-dimensional (3D) seismic data. The submarine canyon is close to the Huaguang depression and herein named as Huaguang Canyon. Till now the origin and development processes of this submarine canyon have not been revealed, and the interplay of canyon incision, aggradation, lateral migration, and levee deposition are still poorly understood. Therefore, the aims of this paper are to: (1) analyze the detailed internal architecture of Huaguang Canyon; (2) investigate the main controlling factors responsible for its formation and evolution; (3) discuss the implications of the Huaguang Canyon for hydrocarbon exploration on the northwest South China Sea margin. Results from this study may contribute to an improved understanding of the stratigraphy and evolution of submarine canyons in carbonate environment on other continental margins worldwide.

2 Geological setting

The South China Sea (SCS) is the largest and deepest marginal sea in the western Pacific with an area of 3.5×10^6 km^2 and its evolution has been jointly affected by the Eurasian, Pacific and Australi-India plates. During the Cenozoic, the South China Sea experienced complex tectonic evolution (e.g., Lüdmann et al., 2001; Yan et al., 2006; Xie et al., 2006; Sibuet et al., 2016). The seafloor spreading initially started at ~33 Ma in the northeastern South China Sea (Li et al., 2015). The spreading center jumped ~20 km southwards and triggered a second phase of spreading in the southwest subbasin at ~23.6 Ma (Li et al., 2015). The seafloor spreading stopped at ~15 Ma in the east subbasin and ~16 Ma in the southwest subbasin (Li et al., 2015).

The Qiongdongnan Basin is a northeast trended Cenozoic sedimentary basin in the northern South China Sea which is bounded to the west by the offshore Red River fault and the NW-elongated Yinggehai-Song Hong Basin, to the east by the Shenhu Uplift and the Zhujiang River Mouth Basin, to the north by Hainan Island and to the south by the Xisha block (Figs 1 and 2) (Clift and Sun, 2006; Zhu et al., 2009; Van Hoang et al., 2010; Zhao et al., 2018). It developed on the western end of the northern rifted continental margin of the South China Sea. Four units can be identified in the Qiongdongnan Basin, including the northern depression, the central uplift, the central depression and the southern uplift arranged from north to south. The evolution of the Qiongdongnan Basin generally underwent two stages, i.e., rift stage and post-rift thermal subsidence stage (Ru and Pigott, 1986). During the rifting stage, a series of half-grabens and sags were developed. Ledong Sag, Lingshui Sag, Songnan Sag, Beijiao Sag, Baodao Sag and Changchang Sag arrange from west to east in the central depression of the Qiongdongnan Basin (Zhang et al., 2013). Additionly, the half-grabens are mainly distributed in the Lingshui Sag, Songnan Sag, and Beijiao Sag, which are bordered by long faults with large vertical offsets (Zhang et al., 2013). Following the rifting stage, the Qiongdongnan Basin experienced post-rift thermal subsidence until the present day and a thick sequence of marine sediments that were dominated by mudstones deposited since Miocene. The basement of the Qiongdongnan Basin mainly consists of Palaeozoic meta-sedimentary rock, which was deformed by Jurassic-Cretaceous granitic intrusions (Zhou et al., 1995). Five sequences can be recognized from seismic stratigraphy in Qiongdongnan Basin in the Neogene. They are the Sanya formation, the Meishan formation, the Huangliu formation, the Yinggehai formation and the Ledong formation, from lower to upper respectively (Fig. 3) (Wu et al., 2009).

The study area is located in the Qiongdongnan Basin and water depth ranges from –200 m to –2 000 m (Figs 1 and 2). The Neogene sediments in the study area are mainly from Indochina (mainly terrigenous clastics), Guangle Uplift and Xisha Uplift (mainly carbonate) (Wu et al., 2009; Sun et al., 2010). The Xisha Islands, comprising more than 40 islands and reefs, are located in the northwest part of the South China Sea. The Xisha Platform was initiated on the Xisha Uplift during the early Miocene (Wu et al., 2014). The Xisha Uplift was subaerially exposed prior to the Miocene, but subsided during the late Oligocene to early Miocene period of seafloor spreading (Wu et al., 2014). The Xisha carbonate platform was formed of fault-bounded blocks that developed during the Xisha Uplift (Wu et al., 2014). The carbonate deposition was initiated at the beginning of the Miocene and flourished throughout the middle Miocene before waning during the late Miocene. The platform was drowned and significantly reduced in size during Pliocene-Quaternary times (Zhao and Zheng, 2010; Wu et al., 2014; Kuang et al., 2014; Shao et al., 2017a, b). The Guangle Uplift is a palaeo-basement high, already existing prior to the Neogene (Fyhn et al., 2009). The Guangle Uplift is

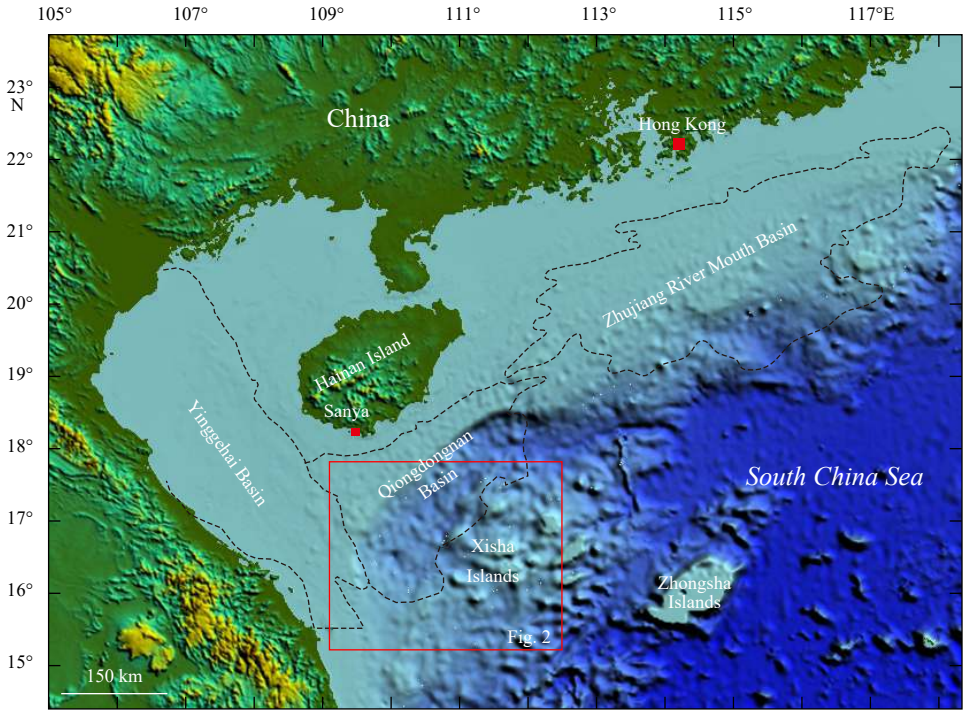

Fig. 1. Location map of the study area in the Qiongdongnan Basin on the northwestern South China Sea margin. The black dotted lines present the boundaries of the Zhujiang River Mouth Basin, the Qiongdongnan Basin and the Yinggehai Basin. The red box indicates the location of Fig. 2. Major topographical features, including Hainan Island, Xisha Islands and Zhongsha Islands are marked.

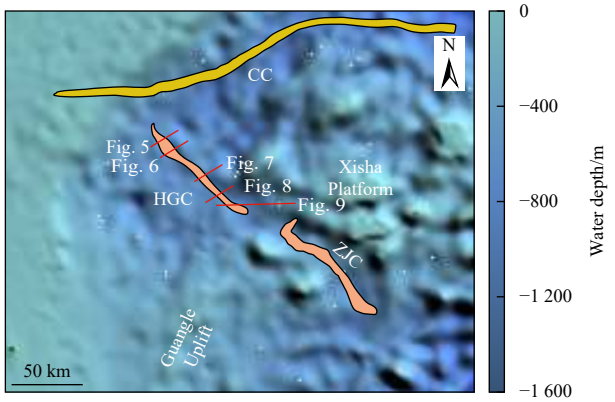

Fig. 2. Distributions of submarine channels on the northwestern South China Sea. The Xisha Platform in the eastern of the HGC. The red lines indicate the seismic profiles in Figs 5, 6, 7, 8 and 9. HGC: Huaguang Canyon, ZJC: Zhongjian Canyon, and CC: Central Canyon.

separated from the Indochina Block through a narrow but very deep intrabasinal depression (Fyhn et al., 2009). The sequences in the Guangle Uplift are characterized by widespread carbonate deposits from early Miocene (Xie et al., 2006; Fyhn, et al., 2009; Sun et al., 2011). The Neogene sequence stratigraphy can be divided into five formations (Xie et al., 2006; Yao et al., 2008; Sun et al., 2010; Wu et al., 2009). They are the Sanya formation (early Miocene), the Meishan formation (middle Miocene), the Huangliu formation (late Miocene), the Yinggehai formation (Pliocene) and the Ledong formation (Pleistocene-Holocene) (Fig. 3).

3 Data and methods

The seismic interpretation carried out as part of this study used high-quality 169 industrial 3D marine seismic data acquired in 2011 by WesternGeco Geophysical 170 Company. The data were processed by the Bureau of Geophysical Prospecting (BGP). The 171 data processing included static corrections, true amplitude recovery, surface related 172 multiple elimination (SRME), radon-transform, velocity analysis, migration, and stack. The dataset used in this study consist of industrially acquired 2D and 3D multi-channel seismic reflection data. The 3D seismic data set has common depth point (CDP) distance and line spacing of 12.5 m and 25 m, respectively. The dominant frequency for the intervals of interest is 40–60 Hz, yielding a vertical seismic resolution of 8–11 m. The 2D seismic profiles have a dominant frequency of ca. 35 Hz and common middle point (CMP) intervals of 6.25 m and 12.5 m. The 2D seismic data have a vertical seismic resolution of ~13 m in the target intervals. The exploration Well YC35-1 was drilled in the lower slope area, and is used to establish the seismic sequence stratigraphic framework. Five seismic sequences can be recognized from seismic stratigraphy of Well YC35-1 since early Miocene, and these sequences have been published by many other literatures (Yuan et al., 2009; Gong et al., 2011; Wang et al., 2014). These sequences are the Sanya formation, Meishan formation, Huangliu formation, Yinggehai formation and Ledong formation, from lower to upper respectively. The sequences are bounded by five seismic reflectors, i.e., T60, T50, T40, T30 and T20 (Wu et al., 2009). Three main reflection horizons (T20, T30 and T40) are used in this study, which have ages of 1.9 Ma, 5.5 Ma and 10.5 Ma, respectively. The Huaguang Canyon was mainly developed at the early stage of Huangliu formation (T40). Sediment fillings and erosional features of Huaguang Canyon can be observed in these three main reflectors.

4 Results

4.1 *Distribution of the Huaguang Canyon*

High-resolution 2D and 3D seismic data show that the buried

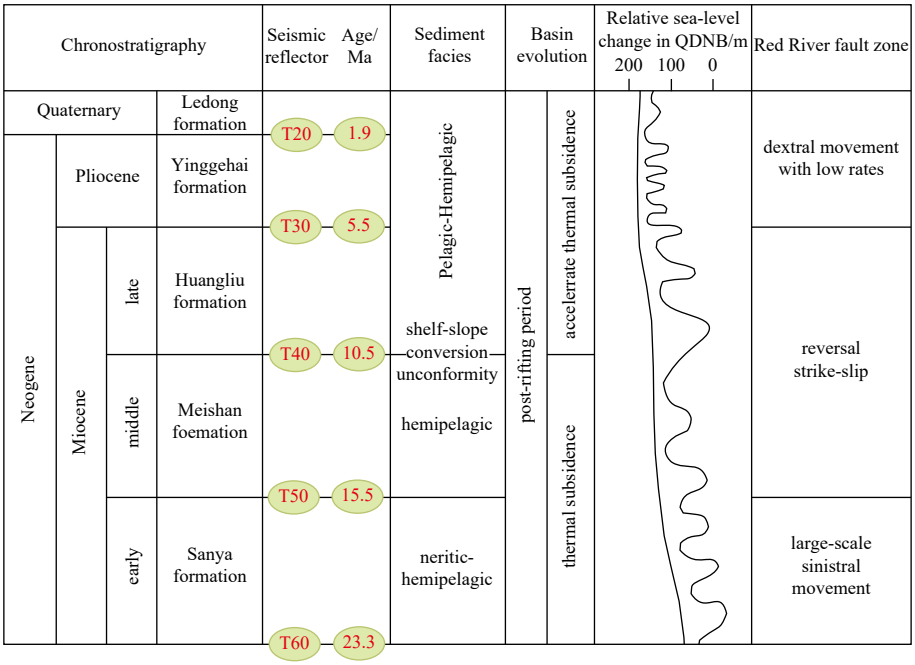

Fig. 3. The Chronostratigraphy profile of the Qiongdongnan Basin from Neogene to Quaternary. The sea level change of Qiongdongnan Basin (QDNB) and global eustatic were adopted from Haq et al. (1987).

Huaguang Canyon is located in the northwest South China Sea margin. It is confined in the Qiongdongnan Basin and does not erode the shelf edge (Fig. 4). The head of the Huaguang Canyon is closed to the Xisha Islands and located between the Xisha Islands and Huaguang depression, with Guangle Uplift to the south (Fig. 4). The lower reach of this canyon is connected to the central canyon. The Huaguang Canyon displays two distinct trends in different areas (Fig. 4). It has NW orientation in the upper reach with a width between 2.5 km and 5 km (Figs 5–8), and it turns to NNW in the lower reach and its width ranges from 4.6 km to 9.5 km (Figs 5 and 6). The length of Huaguang Canyon is of ~140 km and it covers an area of 315 km^2 (Fig. 4). Furthermore,

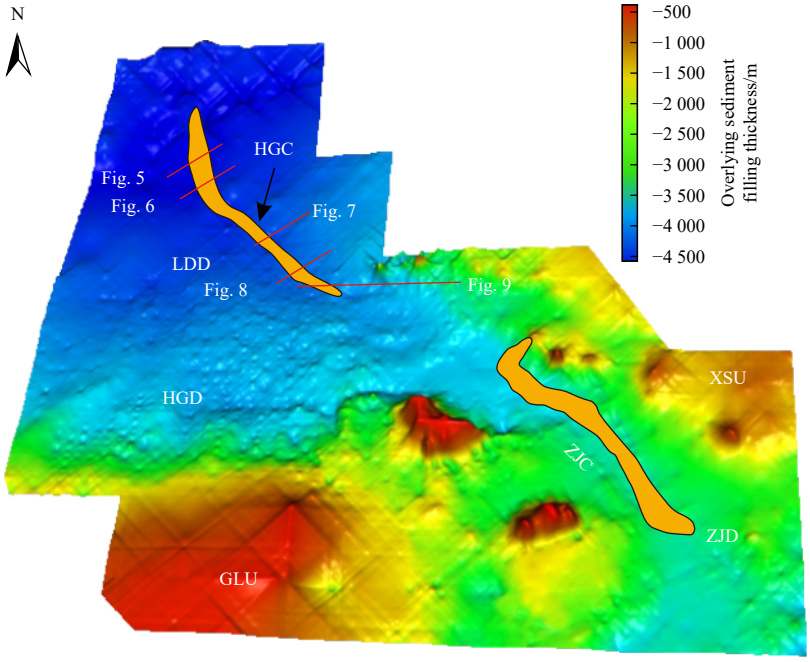

Fig. 4. The paleogeomorphic map of study area in later Miocene with overlying sediment filling thickness ranging from –4 500 m to –500 m. The red lines indicate the seismic profiles in Figs 5, 6, 7, 8 and 9. The orange area in the northwestern of the map denotes the Huaguang Canyon (HGC), and the orange regions in the southeastern of the map indicate the Zhongjian Canyon (ZJC). HGD: Huaguang depression, XSU: Xisha uplift, ZJD: Zhongjian depression, GLU: Guangle uplift, LDD: Ledong depression, and ZJC: Zhongjian Canyon.

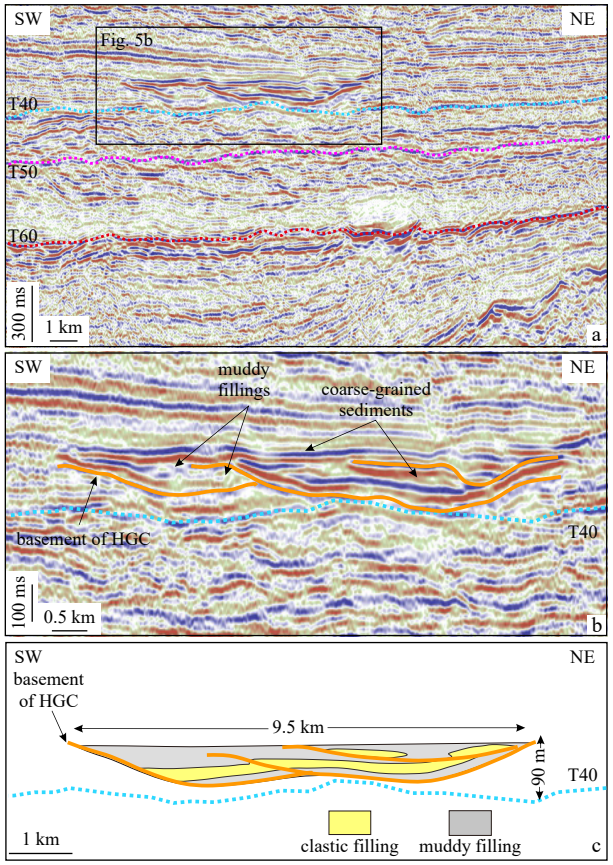

Fig. 5. Cross-sectional seismic profiles across the lower reach of Huaguang Channel (HGC) (a), the buried channels lies in the middle area of the seismic profile (b), and the sketch profile shows deposits buried in the Huaguang Channel (c). Locations of seismic profiles are shown in Fig. 2. The Huaguang Channel is 9.5 km in width and 90 m in depth. The black box in a indicates the buried channels in b, the orange line in b indicates the basement of Huaguang Channel, the yellow section in c indicates the clastic fillings and grey indicates the muddy fillings.

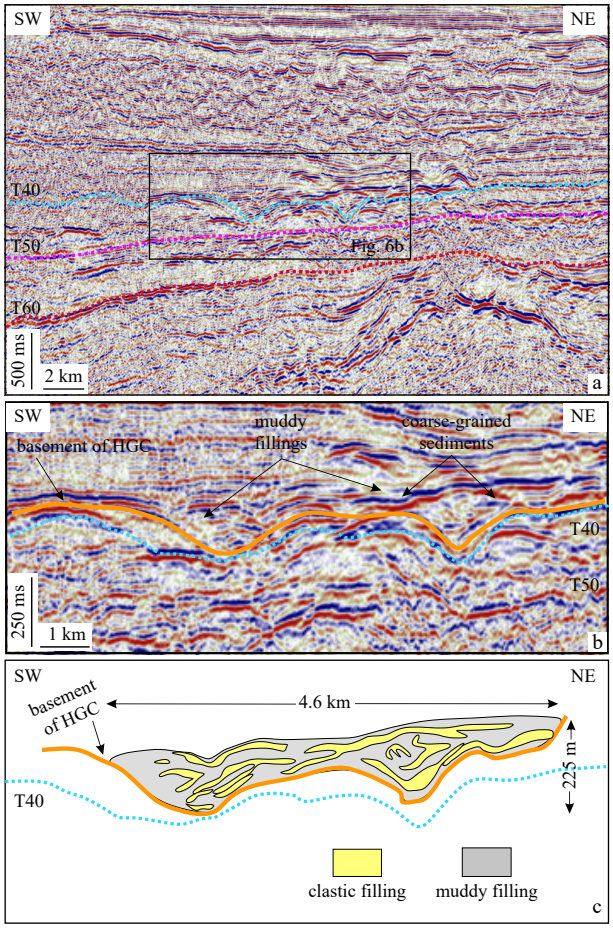

Fig. 6. Cross-sectional seismic profiles across the middle reach of Huaguang Channel (HGC) (a), the buried channels are located in the upper region of the seismic profile (b), and the sketch profile shows deposits buried in the Huaguang Channel (c). Locations of seismic profiles are shown in Fig. 2. The Huaguang Channel is 4.6 km in width and 225 m in depth. The black box in a indicates the buried channels in Fig. 6b, the orange line in b indicates the basement of Huaguang Channel, the yellow section in c indicates the clastic fillings and grey indicates the muddy fillings.

this canyon is buried at depths of 1–2 km below the seafloor and its incision depth ranges from 90 m to 375 m.

4.2 *Internal architecture of the Huaguang Canyon*

The high-resolution seismic data enables the detailed investigation of the internal architectures of the Huaguang Canyon. The strata in the late Miocene is rather complex and shows obvious discontinuous reflectors. Several pronounced seismic bodies can be observed, which are bounded by erosional surfaces. The erosional surfaces are outlined by truncations of underlying seismic reflectors. The deposits filled the buried submarine canyon are characterized as high-amplitude seismic reflections, which might represent sandy deposits in the basal lags, deposited rapidly dumping from high-density turbidity currents (Figs 5–8). Seismic facies exhibit low seismic amplitudes, discontinuous reflections may indicate muddy fillings which reconstructs the top sand deposits.

Obvious differences can be observed in four seismic sections crossing the Huaguang Canyon from its upper to the lower reach (Fig. 4). Obvious erosional features can be observed from palaeogeomorphology in the boundary of Huangliu formation (T40) (Figs 7 and 8). These characteristics indicate the occurrence of erosion and the instability of basement in Huaguang Canyon. The seismic profile crossing the upper reach of Huaguang Canyon shows two V-shaped erosional surfaces, which indicates that the early stage of the canyon consists of two isolated channels, and the formation time of buried channels is in the early stage of late Miocene (Fig. 8). These two buried channels have a deep incision depth into the underlying layers with a distance of ~1.3 km between the two channels (Fig. 8). Seismic reflections are not continuous and cannot be traced in the canyon axis, which can be observed in the cross-sectional profile, while the canyon flank shows continuous and distinct reflections (Fig. 8). The amplitude within the channels is relatively high (Fig. 8). In addition, a normal fault can be identified under the channels (Figs 7 and 8). Further downstream, the lower reach shows two broad, flat, and U-shape cross sections. The width of the buried canyon ranges from 2.5 km to 9.5 km and their depth ranges from 90 m to 375 m (Figs 5–8). The seismic facies in the canyon thalweg are expressed as chaotic packages with high amplitude discontinuous reflections, which can be easily identified in the

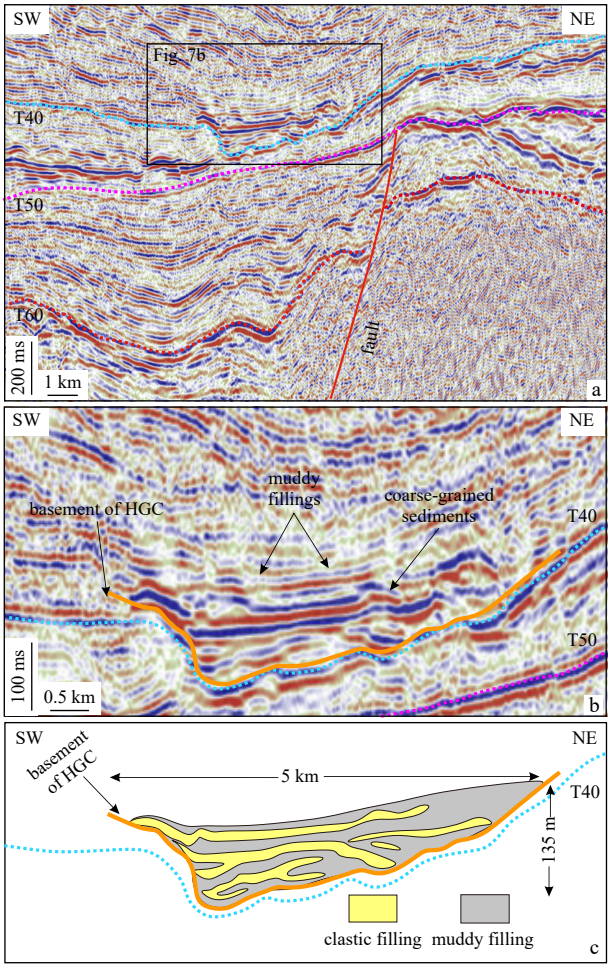

Fig. 7. Cross-sectional seismic profiles across the upper reach of HuaGuang Channel (HGC) (a), the seismic profile shows that the buried channels are distributed near the upper reach (b), and the sketch profile show deposits buried in the Huaguang Channel (c). Locations of seismic profiles are shown in Fig. 2. The Huaguang Channel is 5 km in width and 135 m in depth. The black box in a indicates the buried channels in Fig. 7b, the orange line in b indicates the basement of Huaguang Channel, the yellow section in c indicates the clastic fillings and grey indicates the muddy fillings.

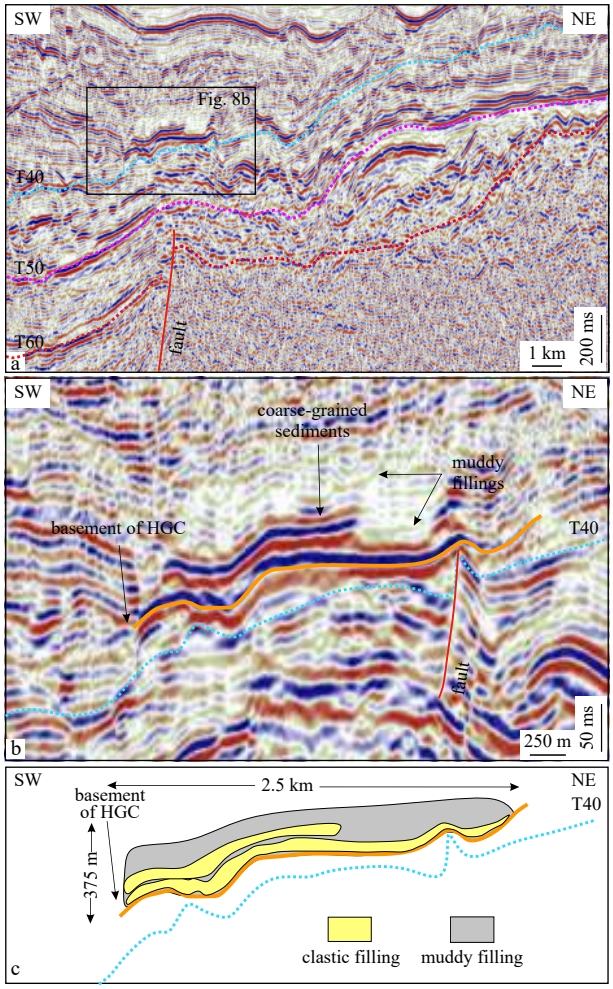

Fig. 8. Cross-sectional seismic profiles across the upper reach of HuaGuang Channel (HGC) (a), the buried channels are closed to the southwestern area of the seismic profile (b), and the sketch profile show deposits buried in the Huaguang Channel (c). Locations of seismic profiles are shown in Fig. 2. The Huaguang Channel is 2.5 km in width and 375 m in depth. The black box in a indicates the buried channels in Fig. 8b, the orange line in b indicates the basement of Huaguang Channel, the yellow section in c indicates the clastic fillings and grey indicates the muddy fillings.

canyon axis (Fig. 4). They commonly display len-shaped, concave-up cross-sectional geometry and are typically contained within a U-shaped basal erosional surface, where clear truncation terminations below and onlap terminations above (Fig. 4). From upper reach to lower reach of the Huaguang Canyon, the width/depth ratios of the buried canyon gradually increased (Figs 5–8).

5 Discussion

5.1 *Controlling factors on the initiation and development of the Huaguang Canyon*

Multiple causes have been proposed to explain the origin of submarine canyons, while the erosion of the slope is considered as the most principal reason (Shepard, 1981). The erosion of slope is mainly resulted in mass wasting events and turbidity currents. The headward erosion driven by sediment flow down-cutting are the precursors of submarine canyon systems (Pratson and Coakley, 1996; Harris and Whiteway, 2011). Slope failures have also been considered as the most common process responsible for the initiation of submarine canyons. They are formed by retrogressive erosion from the initial slide scar and the erosional events can progressively migrate upslope or downslope (Twichell and Robert, 1982; Pratson and Coakley, 1996). Submarine canyons controlled by slope failure has been documented in several areas, such as the Diepgat canyon on the northern KwaZulu-Natal continental shelf, South Africa (Green and Uken, 2008). In addition, tectonic activities (e.g., faults, uplift and denudation of basins) are also regarded as the main factors influencing the origin and development of the submarine canyons. It has been identified in the submarine Mona Canyon which between Puerto Rico and Hispaniola of the Greater Antilles, and the Zhongjian Canyon in the northwest South China Sea (Mondziel et al., 2010; Lu et al., 2018). Furthermore, the initiation and development of submarine canyons are also controlled by the drops of sea-level, because glacial troughs incised into the continental shelf by gla-

cial erosion during sea level lowstands. Several areas have documented this mechanism responsible for submarine canyons, such as the Canyon of the Indus River-Fan system and canyon in the western Gulf of Lion, the western Mediterranean Sea (Baztan et al., 2005; Clift et al., 2014).

In this study, the head of the Huaguang Canyon is closed to the Xisha Island, where few rivers have been reported. Thus the initiation and development of submarine canyons under the effect of river sediment input is not possible. In addition, based on the interpreted seismic lines, there is no evidence of slope failures (Figs 5–8). Thus, slope failure is not the main reason for interpreting the origin of the Huaguang Canyon. In terms of eustatism, a significant drop of sea-level in the study area can be observed at the early stage of late Miocene from the chronostratigraphy profile (Fig. 3). The erosional processes of submarine canyons are associated to eustatic lowering enhanced by local tectonics (Lofi and Berné, 2008), and the period of Huaguang Canyon initiation is corresponding to the most pronounced sea-level drop at the early stage of late Miocene (10.5 Ma) (Figs 3 and 5–8). Additionally, several erosional features can be observed in palaeogeomorphology in the boundary T40 (Figs 7 and 8). These erosion characteristics indicate that the instability of basement of Huaguang Canyon. Therefore, we propose that Huaguang Canyon is ascribed to the erosion by gravity flows during sea-level lowstands. Moreover, the enlargement of canyon width of Huaguang Canyon (2.5 km in head to 9.5 km in tail) indicates that the lateral migration has a great effect on the development in this area (Figs 5c and 8c). From the internal architecture of the Huaguang Canyon, the channels were buried quickly by sediment after its formation (Figs 5–8). The possibility of sediment from the rivers can be excluded because few rivers is adjacent to the head of the Huaguang Canyon. Extensive carbonate platforms developed in the middle Miocene and they are drowned during the late Miocene (Wu et al., 2014). But the isolated carbonate platform in the central Xisha uplift continued to develop to present. In the early stage of Late Miocene, the Xisha carbonate platform exposed, producing huge amounts of carbonate detritus, which could act as the sediment source (Lu et al., 2018). The progradation reflections and some erosional features have been identified in Fig. 9, which indicate that the Huaguang Channel is supplied from the Xisha carbonate platform. Therefore, we propose that the deposits in the canyon fills are mainly sourced from the Xisha carbonate platform. With regard to the clastic content in the buried sediments of Huaguang Canyon, more work needed to improve the understanding of them in the future.

5.2 *Comparison with other submarine canyons on the northwest South China Sea margin*

In contrast to the central canyon and Zhongjian Canyon in the northwest South China Sea, the Huaguang Canyon has several different characteristics in terms of canyon scales, formation time, and the sources of sediment supply. This may give us a better understanding on the evolution of this ancient submairne canyon. The central canyon in the Qiongdongnan Basin is located at the abyssal environment with a slope subparallel orientation. It is about 570 km in length and 4–8 km in width, and no canyons or gullies are observed adjacent to the central canyon (Yuan et al., 2009). The central canyon is proposed to be dominated by both the large-scale submarine gravity flow (slumps, debris flows or turbidite currents) incision and tectonic activities (Su et al., 2014). However, the forming mechanisms in three segments of this canyon (the head of the canyon, the western of the canyon and the eastern of the canyon) are different (Su et al., 2014). The head area of the canyon was triggered by the abundant sediment supply from western source (the Red River system or the eastern Vietnam or the Hainan Island) together with the fault activity the Red River Fault (5.7 Ma). The eastern part of the canyon is influenced by the tectonic transformation at the end of the middle Miocene (11.6 Ma). The evolution of the canyon in the western segment should be affected by the combination of the turbidite channel from western source, the mass transport complex from the northern continental slope (Su et al., 2014). In addition, the Zhongjian Canyon is located between two carbonate platforms which developed at the middle Miocene (Wu et al., 2014; Lu et al., 2018). The Zhongjian Canyon is approximately 9 km in width and maximum 125 km in length (Lu et al., 2018). The Zhongjian Canyon originated from NW-SE strike-slip fault activities during syn-rift and post-rift stages, and grew during the development of Xisha carbonate platforms since the middle Miocene (Lu et al., 2018). The water depth of the Zhongjian Canyon increased due to the rapid development of carbonate platforms (Lu et al., 2018). Predominantly mixed carbonate-igneous clasts and muds are the main sediment inputs to the Zhongjian Canyon (Lu et al., 2018).

In our study area, the Huaguang Canyon is about 140 km in length and 2.5–9.5 km in width (Figs 5–8). The scale of this canyon is much smaller than the central canyon and Zhongjian Canyon. The Huaguang Canyon was initiated at the early stage of the late Miocene (10.5 Ma), corresponding to the expansion of carbonate platform in the Xisha uplift (Wu et al., 2014). However, the central canyon and Zhongjian Canyon began to develop at the end of the middle Miocene (11.6 Ma). Therefore, the forma-

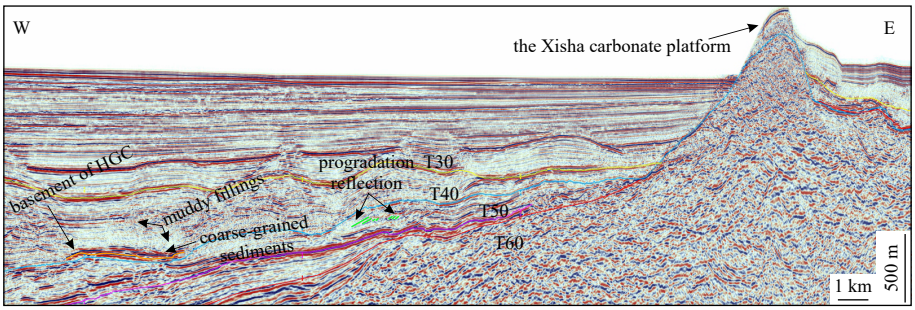

Fig. 9. The seismic profile is shown in Figs 2 and 4. The Xisha carbonate platform and the Huaguang Channel (HGC) are shown in the cross-sectional seismic profile. The orange line indicates the basement of the Huaguang Channel. The green lines represent the progradation reflection. The high-amplitude reflection indicates the clastic fillings and the strong and high reflections indicate the muddy fillings.

tion time of the Huaguang Canyon is later than the central canyon and Zhongjian Canyon. Furthermore, there is a significant difference on the source of sediment supply. The sediment source of the Central canyon is from western (the Red River system or the eastern Vietnam or the Hainan Island) and the northern continental slope (Su et al., 2014). The sediment within the Zhongjian Canyon is supplied from the Xisha and Guangle carbonate platforms (Lu et al., 2018). However, the Huaguang Canyon is only received sediment from the Xisha carbonate platform.

As mentioned above, the Huaguang Canyon has later formation time, smaller width and length, and single source of sediment supply compared to the adjacent large-scale central canyon and Zhongjian Canyon.

5.3 *Significance for hydrocarbon exploration in the northwest South China Sea*

Submarine canyons and channels have been considered as potential areas for hydrocarbon explorations (Clark and Pickering, 1996). The canyon fills accumulating within the submarine canyons play significant roles in reserving oil and gas (Crossey et al., 2006). Coarse-grained, high-density turbidity current deposits are commonly observed in submarine canyons, which are transported from the canyon heads to the deep-water environments (Shepard and Dill, 1966; Normark and Carlson, 2003). The coarse-grained deposits are important architectural elements of submarine-canyon fills, which can serve as hydrocarbon reservoirs (Anderson et al., 2006). This phenomenon has been documented in many other regions, such as the San Joaquin Basin in California where large amounts of oil are buried in sand-rich, coarse-grained, high-density turbidity current deposit sequences closely associated with submarine canyons (Lamb et al., 2003). Furthermore, marginal reef carbonate platforms in offshore areas can deliver large amounts of coarse-grained sediments to the submarine canyons (Puga-Bernabéu et al., 2008). During the period of sea-level falls, the occurrence of sand-rich deep-water deposition will increase with sea-level falls sufficient to expose most of the shelf (Posamentier and Kolla, 2003). Coarse-grained, deep-water, carbonate sediment has been recognized as very important and attractive reservoirs for hydrocarbon explorations (Scholle, 1977). These carbonate reservoirs have been documented in several regions around the world, such as the carbonates from the Otway Basin in Australia (Leach and Wallace, 2001).

In this case, the sediment trapped within the Huaguang Canyon is mainly sourced from the Xisha carbonate platform (Fig. 9). The high amplitude reflections within the canyon fills indicate the presence of carbonate clastic fillings, and the muddy fillings are considered as regional caps (Figs 5–8). Comparing with other submarine canyons in Qiongdongnan Basin like the central canyon, large amounts of turbidite channel sediments were buried in this canyon during the period from 5.5 Ma to 3.8 Ma (Wang, 2012). These coarse-grained debris flow deposits have been identified as good reservoir for hydrocarbon exploration in deep water environment (Wang, 2012). The Huaguang Canyon was initiated and formed at the early stage of late Miocene, corresponding to a sea-level drop. And this will increase the delivery of coarse-grained deposits from the Xisha carbonate platform to the head area of Huaguang Canyon. Therefore, the Huaguang Canyon would have received significant amount carbonate sediment from the Xisha carbonate platform during sea-level lowstands at the late Miocene, which may be considered potential area for hydrocarbon explorations on the northwest South China Sea margin.

6 Conclusions

High-resolution multichannel seismic data allows us to investigate a previous, undocumented submarine canyon (Huaguang Canyon) in the northwest South China Sea. Results of seismic interpretation provides new information for the better understanding of the formation time and development of Huaguang Canyon. The main conclusions of this work are as follows:

(1) The Huaguang Canyon is located in the Qiongdongnan Basin, northwest South China Sea, and it is closed to the Xisha carbonate platform. The Huaguang Canyon with a NW orientation is 140 km in length, where 2.5 km to 5 km in width in its upper reach and 4.6 km to 9.5 km in width in its lower reach.

(2) The Huaguang Canyon was initiated and formed at the early stage of the late Miocene (10.5 Ma). The origin of Huaguang Canyon is corresponding to a significant drop of the sea-level at the late Miocene. The lowering of sea-level resulted in significant erosion and frequent gravity flows close to the Xisha carbonate platform.

(3) The Huaguang Canyon shows later formation time, smaller width and length, and single source of sediment supply (from the Xisha carbonate platform) comparing to other adjacent large-scale submarine canyons (Central Canyon and Zhongjian Canyon).

(4) The Huaguang Canyon was buried by coarse-grained carbonate sediment sourced from the Xisha carbonate platform. These coarse-grained sediments are regarded as reservoir rocks and the muddy fillings are considered as the regional caps. And this canyon may be considered as a potential area for future hydrocarbon exploration on the northwest South China Sea margin.

References

Anderson K S, Graham S A, Hubbard S M. 2006. Facies, architecture, and origin of a reservoir-scale sand-rich succession within submarine canyon fill: insights from wagon caves rock (paleocene), Santa Lucia range, California, U.S.A.. Journal of Sedimentary Research, 76(5): 819–838, doi: 10.2110/jsr.2006.066

Baztan J, Berné S, Olivet J L, et al. 2005. Axial incision: the key to understand submarine canyon evolution (in the western Gulf of Lion). Marine and Petroleum Geology, 22(6–7): 805–826

Bouma A H. 2004. Key controls on the characteristics of turbidite systems. Geological Society, London, Special Publications, 222(1): 9–22, doi: 10.1144/GSL.SP.2004.222.01.02

Clark J D, Pickering K T. 1996. Architectural elements and growth patterns of submarine channels: application to hydrocarbon exploration. AAPG Bulletin, 80(2): 194–221

Clift P D, Giosan L, Henstock T J, et al. 2014. Sediment storage and reworking on the shelf and in the Canyon of the Indus River-Fan System since the last glacial maximum. Basin Research, 26(1): 183–202

Clift P D, Sun Zhen. 2006. The sedimentary and tectonic evolution of the Yinggehai-Song Hong Basin and the southern Hainan margin, South China Sea: implications for Tibetan uplift and monsoon intensification. Journal of Geophysical Research: Solid Earth, 111(B6): B06405

Cossu R, Wells M G. 2013. The evolution of submarine channels under the influence of Coriolis forces: experimental observations of flow structures. Terra Nova, 25(1): 65–71

Crossey L J, Fischer T P, Patchett P J, et al. 2006. Dissected hydrologic system at the Grand Canyon: Interaction between deeply derived fluids and plateau aquifer waters in modern springs and travertine. Geology, 34(1): 25–28, doi: 10.1130/G22057.1

de Leeuw J, Eggenhuisen J T, Cartigny M J B. 2016. Morphodynamics of submarine channel inception revealed by new experimental approach. Nature Communications, 7: 10886

Ding Weiwei, Li Jiabiao, Li Jun, et al. 2013. Morphotectonics and evolutionary controls on the Pearl River Canyon system, South China Sea. Marine Geophysical Research, 34(3–4): 221–238

Feng Jingchun, Wang Yi, Li Xiaosen, et al. 2015. Production performance of gas hydrate accumulation at the GMGS2-Site 16 of the Pearl River Mouth Basin in the South China Sea. Journal of Natural Gas Science and Engineering, 27: 306–320, doi: 10.1016/j.jngse.2015.08.071

Fyhn M B W, Nielsen L H, Boldreel L O, et al. 2009. Geological evolution, regional perspectives and hydrocarbon potential of the northwest Phu Khanh Basin, offshore Central Vietnam. Marine and Petroleum Geology, 26(1): 1–24, doi: 10.1016/j.marpetgeo.2007.07.014

Gong Chenglin, Wang Yingmin, Zhu Weilin, et al. 2011. The Central Submarine Canyon in the Qiongdongnan Basin, northwestern South China Sea: architecture, sequence stratigraphy, and depositional processes. Marine and Petroleum Geology, 28(9): 1690–1702, doi: 10.1016/j.marpetgeo.2011.06.005

Green A, Uken R. 2008. Submarine landsliding and canyon evolution on the northern KwaZulu-Natal continental shelf, South Africa, SW Indian Ocean. Marine Geology, 254(3–4): 152–170

Haq B U, Hardenbol J A N, Vail P R. 1987. Chronology of fluctuating sea levels since the Triassic. Science, 235(4793): 1156–1167, doi: 10.1126/science.235.4793.1156

Harris P T, Whiteway T. 2011. Global distribution of large submarine canyons: geomorphic differences between active and passive continental margins. Marine Geology, 285(1–4): 69–86

Kolla V. 2007. A review of sinuous channel avulsion patterns in some major deep-sea fans and factors controlling them. Marine and Petroleum Geology, 24(6–9): 450–469

Kuang Zenggui, Zhong Guangfa, Wang Liaoliang, et al. 2014. Channel-related sediment waves on the eastern slope offshore Dongsha Islands, northern South China Sea. Journal of Asian Earth Sciences, 79: 540–551, doi: 10.1016/j.jseaes.2012.09.025

Lüdmann T, Wong H K, Wang Pinxian. 2001. Plio–Quaternary sedimentation processes and neotectonics of the northern continental margin of the South China Sea. Marine Geology, 172(3–4): 331–358

Lamb M A, Anderson K S, Graham S A. 2003. Stratigraphic Architecture of A Sand-Rich, Deep-Sea Depositional System: the Stevens Sandstone, San Joaquin Basin, California. California: Pacific Seciton AAPG Publication

Leach A S, Wallace M W. 2001. Cenozoic submarine canyon systems in cool water carbonates from the Otway Basin, Victoria, Australia. In: Hill K C, Bernecker T, eds. Eastern Australasian Basins Symposium, A Refocused Energy Perspective for the Future. Petroleum Exploration Society of Australia Special Publication, 1: 465–473

Li Xiangquan, Fairweather L, Wu Shiguo, et al. 2013. Morphology, sedimentary features and evolution of a large palaeo submarine canyon in Qiongdongnan Basin, northern South China Sea. Journal of Asian Earth Sciences, 62: 685–696, doi: 10.1016/j.jseaes.2012.11.019

Li Chunfeng, Li Jiabiao, Ding Weiwei, et al. 2015. Seismic stratigraphy of the central South China Sea basin and implications for neotectonics. Journal of Geophysical Research: Solid Earth, 120(3): 1377–1399, doi: 10.1002/2014JB011686

Lofi J, Berné S. 2008. Evidence for pre-Messinian submarine canyons on the Gulf of Lions slope (Western Mediterranean). Marine and Petroleum Geology, 25(8): 804–817, doi: 10.1016/j.marpetgeo.2008.04.006

Lu Yintao, Li Wei, Wu Shiguo, et al. 2018. Morphology, architecture, and evolutionary processes of the Zhongjian Canyon between two carbonate platforms, South China Sea. Interpretation, 6(4): SO1–SO15

Mayall M, Jones E, Casey M. 2006. Turbidite channel reservoirs—Key elements in facies prediction and effective development. Marine and Petroleum Geology, 23(8): 821–841

McHargue T, Pyrcz M J, Sullivan M D, et al. 2011. Architecture of turbidite channel systems on the continental slope: patterns and predictions. Marine and Petroleum Geology, 28(3): 728–743, doi: 10.1016/j.marpetgeo.2010.07.008

Mondziel S, Grindlay N, Mann P, et al. 2010. Morphology, structure, and tectonic evolution of the Mona canyon (northern Mona passage) from multibeam bathymetry, side-scan sonar, and seismic reflection profiles. Tectonics, 29(2): TC2003

Normark W R, Carlson P R. 2003. Giant submarine canyons: Is size any clue to their importance in the rock record?. In: Chan M A, Archer A W, eds. Extreme Depositional Environments: Mega end Members in Geologic Time. Boulder: Geological Society of America, 370: 175–190

Ortiz-Karpf A, Hodgson D M, Mccaffrey W D. 2015. The role of mass-transport complexes in controlling channel avulsion and the subsequent sediment dispersal patterns on an active margin: the Magdalena Fan, offshore Colombia. Marine and Petroleum Geology, 64: 58–75, doi: 10.1016/j.marpetgeo.2015.01.005

Peakall J, Kane I A, Masson D G, et al. 2012. Global (latitudinal) variation in submarine channel sinuosity. Geology, 40(1): 11–14, doi: 10.1130/G32295.1

Piper D J W, Normark W R. 1983. Turbidite depositional patterns and flow characteristics, Navy Submarine Fan, California Borderland. Sedimentology, 30(5): 681–694, doi: 10.1111/j.1365-3091.1983.tb00702.x

Posamentier H W, Kolla V. 2003. Seismic geomorphology and stratigraphy of depositional elements in deep-water settings. Journal of Sedimentary Research, 73(3): 367–388, doi: 10.1306/111302730367

Pratson L F, Coakley B J. 1996. A model for the headward erosion of submarine canyons induced by downslope-eroding sediment flows. GSA Bulletin, 108(2): 225–234, doi: 10.1130/0016-7606(1996)108<0225:AMFTHE>2.3.CO;2

Puga-Bernabéu A, Martín J M, Braga J C. 2008. Sedimentary processes in a submarine canyon excavated into a temperate-carbonate ramp (Granada Basin, southern Spain). Sedimentology, 55(5): 1449–1466, doi: 10.1111/j.1365-3091.2008.00952.x

Richards M, Bowman M, Reading H. 1998. Submarine-fan systems i: characterization and stratigraphic prediction. Marine and Petroleum Geology, 15(7): 689–717, doi: 10.1016/S0264-8172(98)00036-1

Ru Ke, Pigott J D. 1986. Episodic rifting and subsidence in the South China Sea. AAPG Bull, 70(9): 1136–1155

Scholle P A. 1977. Chalk diagenesis and its relation to petroleum exploration: oil from chalks, a modern miracle?. AAPG Bulletin, 61(7): 982–1009

Shao Lei, Cui Yuchi, Qiao Peijun, et al. 2017a. Sea-level changes and carbonate platform evolution of the Xisha Islands (South China Sea) since the Early Miocene. Palaeogeography, Palaeoclimatology, Palaeoecology, 485: 504–516, doi: 10.1016/j.palaeo.2017.07.006

Shao Lei, Li Qianyu, Zhu Weilin, et al. 2017b. Neogene carbonate platform development in the NW South China Sea: litho-, bio- and chemo-stratigraphic evidence. Marine Geology, 385: 233–243

Shepard F P. 1981. Submarine canyons: multiple causes and long-time persistence. AAPG Bulletin, 65(6): 1062–1077

Shepard F P, Dill R F. 1966. Marine Geology. (Book Reviews: Submarine Canyons and Other Sea Valleys). Science, 154(3755): 1433–1434, doi: 10.1126/science.154.3755.1433

Sibuet J C, Yeh Y C, Lee C S. 2016. Geodynamics of the South China Sea. Tectonophysics, 692: 98–119

Su Ming, Xie Xinong, Xie Yuhong, et al. 2014. The segmentations and the significances of the Central Canyon System in the Qiongdongnan Basin, northern South China Sea. Journal of Asian Earth Sciences, 79: 552–563, doi: 10.1016/j.jseaes.2012.12.038

Sun Qiliang, Wu Shiguo, Hovland M, et al. 2011. The morphologies and genesis of mega-pockmarks near the Xisha Uplift, South China Sea. Marine & Petroleum Geology, 28(6): 1146–1156

Sun Qiliang, Wu Shiguo, Lü Fuliang, et al. 2010. Polygonal faults and their implications for hydrocarbon reservoirs in the southern Qiongdongnan Basin, South China Sea. Journal of Asian Earth Sciences, 39(5): 470–479, doi: 10.1016/j.jseaes.2010.04.002

Twichell D C, Roberts D G. 1982. Morphology, distribution, and development of submarine canyons on the United States Atlantic continental slope between Hudson arid Baltimore Canyons. Geology, 10(8): 408–412, doi: 10.1130/0091-7613(1982)10<408:

MDADOS>2.0.CO;2

Van Hoang L, Clift P D, Schwab A M, et al. 2010. Large-scale erosional response of SE Asia to monsoon evolution reconstructed from sedimentary records of the Song Hong-Yinggehai and Qiongdongnan Basins, South China Sea. Geological Society, London, Special Publications, 342(1): 219–244, doi: 10.1144/SP342.13

Wang Zhenfeng. 2012. Important deepwater hydrocarbon reservoirs: the central canyon system in the Qiongdongnan Basin. Acta Sedimentologica Sinica (in Chinese), 30(4): 646–653

Wang Xiujuan, Collett T S, Lee M W, et al. 2014. Geological controls on the occurrence of gas hydrate from core, downhole log, and seismic data in the Shenhu area, South China Sea. Marine Geology, 357: 272–292

Wang Ce, Liang Xinquan, Foster D A, et al. 2016. Zircon U-Pb geochronology and heavy mineral composition constraints on the provenance of the middle Miocene deep-water reservoir sedimentary rocks in the Yinggehai-Song Hong Basin, South China Sea. Marine and Petroleum Geology, 77: 819–834, doi: 10.1016/j.marpetgeo.2016.05.009

Wu Shiguo, Yang Zhen, Wang Dawei, et al. 2014. Architecture, development and geological control of the Xisha carbonate platforms, northwestern South China Sea. Marine Geology, 350: 71–83, doi: 10.1016/j.margeo.2013.12.016

Wu Shiguo, Yuan Shengqiang, Zhang Gongcheng, et al. 2009. Seismic characteristics of a reef carbonate reservoir and implications for hydrocarbon exploration in deepwater of the Qiongdongnan Basin, northern South China Sea. Marine and Petroleum Geology, 26(6): 817–823, doi: 10.1016/j.marpetgeo.2008.04.008

Wynn R B, Cronin B T, Peakall J. 2007. Sinuous deep-water channels: genesis, geometry and architecture. Marine and Petroleum Geology, 24(6–9): 341–387

Xie Xinong, Müller R D, Li Sitian, et al. 2006. Origin of anomalous subsidence along the Northern South China Sea margin and its relationship to dynamic topography. Marine and Petroleum Geology, 23(7): 745–765, doi: 10.1016/j.marpetgeo.2006.03.004

Yan Pin, Deng Hui, Liu Hailing, et al. 2006. The temporal and spatial distribution of volcanism in the South China Sea region. Journal of Asian Earth Sciences, 27(5): 647–659

Yao Genshun, Yuan Shengqiang, Wu Shiguo, et al. 2008. Double provenance depositional model and exploration prospect in the deep-water area of Qiongdongnan Basin. Petroleum Exploration and Development, 35(6): 685–691, doi: 10.1016/S1876-3804(09)60101-4

Yuan Shengqiang, Wu Shiguo, Thomas L, et al. 2009. Fine-grained Pleistocene deepwater turbidite channel system on the slope of Qiongdongnan Basin, northern South China Sea. Marine and Petroleum Geology, 26(8): 1441–1451

Zhang Guangxue, Liang Jinqiang, Lu Jingan, et al. 2015. Geological features, controlling factors and potential prospects of the gas hydrate occurrence in the east part of the Pearl River Mouth Basin, South China Sea. Marine and Petroleum Geology, 67: 356–367

Zhang Cuimei, Wang Zhenfeng, Sun Zhipeng, et al. 2013. Structural differences between the western and eastern Qiongdongnan Basin: evidence of Indochina block extrusion and South China Sea seafloor spreading. Marine Geophysical Research, 34(3–4): 309–323

Zhao Zhongxian, Sun Zhen, Sun Longtao, et al. 2018. Cenozoic tectonic subsidence in the Qiongdongnan Basin, northern South China Sea. Basin Research, 30(S1): 269–288

Zhao Yanyan, Zheng Yongfei. 2010. Stable isotope evidence for involvement of deglacial meltwater in Ediacaran carbonates in South China. Chemical Geology, 271(1–2): 86–100

Zhou Di, Ru Ke, Chen Hanzong. 1995. Kinematics of Cenozoic extension on the South China Sea continental margin and its implications for the tectonic evolution of the region. Tectonophysics, 251(1–4): 161–177

Zhu Weilin, Huang Baojia, Mi Lijun, et al. 2009. Geochemistry, origin, and deep-water exploration potential of natural gases in the Pearl River Mouth and Qiongdongnan Basins, South China Sea. AAPG Bulletin, 93(6): 741–761, doi: 10.1306/02170908099